CoFe alloy as middle layer for strong spin dependent quantum well resonant tunneling in MgO double barrier magnetic tunnel junctions

R. S. Liu,[1,*] See-Hun Yang,[1] Xin Jiang,[1] X.-G. Zhang,[2] Charles Rettner,[1] Li Gao,[1] Teya Topuria,[1] Philip M. Rice,[1] Weifeng Zhang,[1] C. M. Canali,[3] and Stuart S. P. Parkin[1]

[1]*IBM Research, Almaden Research Center, 650 Harry Road, San Jose, California 95120, USA*

[2]*Center for Nanophase Materials Sciences and Computer Science and Mathematics Division, Oak Ridge National Laboratory, Oak Ridge, Tennessee 37831-9463, USA*

[3]*School of Computer Science, Physics and Mathematics, Linnaeus University, 391 82 Kalmar, Sweden*

(Received 31 May 2012; published 16 January 2013)

We report on spin dependent quantum well (QW) resonances in the CoFe alloy middle layer of CoFe/MgO/CoFe/MgO/CoFeB double barrier magnetic tunnel junctions. The dI/dV spectra reveal clear resonant peaks for the parallel magnetization configurations, which can be related to the existence of QW resonances obtained from first-principles calculations. We observe that the differential tunneling magnetoresistance (TMR) exhibits an oscillatory behavior as a function of voltage with a sign change as well as a pronounced TMR enhancement at resonant voltages at room temperature. The observation of strong QW resonances indicates that the CoFe film possesses a long majority spin mean-free path, and the substitutional disorder does not cause a significant increase of scattering. Both points are confirmed by first-principles electronic structure calculation.

DOI: 10.1103/PhysRevB.87.024411 PACS number(s): 75.76.+j, 85.75.Mm, 76.50.+g

I. INTRODUCTION

The tunneling magnetoresistance (TMR) effect[1,2] in a magnetic tunnel junction (MTJ), consisting of an FM1/I/FM2 structure where FM1 and FM2 are ferromagnetic layers and I is an insulator, has attracted considerable interest due to its important applications in magnetic random access memories and read heads/sensors. High TMR, desired for such type of applications, has been reported using single MgO barrier MTJs.[3,4] However, TMR drops significantly from the maximum at zero bias with increasing bias voltage, which limits its application in the high bias voltage region. Spin dependent quantum well (QW) resonant tunneling effect in double barrier MTJs (DBMTJs), comprised of FM1/I1/FM2/I2/FM3, has received increasing attention because it may enhance TMR at resonant voltages.[5–7] In an earlier experiment, Nagahama *et al.*[8] observed oscillations in the tunneling conductance of a CoFe/AlOx/Fe/Cr junction due to a QW resonance effect, yet the measured signal was small and could only be seen in the second derivative of the current-voltage curve. More recently, Nozaki *et al.*[9] reported oscillatory differential conductance in epitaxial Fe/MgO/Fe/MgO/Fe DBMTJs,[10] but the nonuniformity of the Fe middle layer due to the island formation on MgO led to only a small oscillation amplitude. Later on, Niizeki *et al.*[11] demonstrated the QW resonant tunneling in fully epitaxial Fe(001)/MgO/ultrathin Fe/Cr MTJs, yet the TMR increase at QW resonance was still subtle at room temperature (RT). Past studies have focused on using pure Fe middle layer[7–13] because of the need to preserve the coherence of electron wave function with Δ_1 symmetry and the belief that pure Fe(100) is best suited for this purpose.[3,14,15] However, the observed QW resonances are weak due to a short majority spin mean-free path (MFP) in the Fe film, which is only about 1–2 nm[16,17] and very close to the film thicknesses. To enhance QW resonance in MgO DBMTJs, it is desirable to incorporate a magnetic middle layer with a long spin MFP as well as a bcc MgO (001)-compatible crystalline structure. Giant TMR was predicted in bcc CoFe(001)/MgO(001)/CoFe(001) MTJs[18] and was observed in similar highly textured structures.[4] Also, CoFe can be grown using simple sputter-deposition techniques at ambient temperature on amorphous substrate layers, which is more suitable for practical applications. In addition, the majority spin MFP in Co is several times longer than that in Fe,[16] hence it may be possible that CoFe (especially Co-rich CoFe) could preserve a longer spin MFP. However, a competing effect of alloying (disorder) may introduce an increase of the overall amount of scattering in CoFe, reducing the MFP and preventing the formation of QW resonances. Therefore, the study of QW resonances in CoFe is very important for developing practical spintronic devices as well as understanding new physics of quantum resonant tunneling in disordered alloys.

In this paper, we report the observation of strong spin dependent QW resonances in the CoFe alloy middle layer of MgO DBMTJs. Our first-principles electronic structure calculation shows that the Fermi energy of the CoFe alloy is completely above the d bands, and there is only a small difference in the s-phase shift between Co and Fe atomic potentials. Thus strong QW resonances in CoFe can be explained in terms of a long majority spin MFP in CoFe. This counterintuitive finding indicates that a pure, single-crystal magnetic material is not indispensable for spin-polarized resonant tunneling.[8,13,19,20]

II. EXPERIMENTS

The DBMTJ film stacks were prepared by magnetron sputtering at ambient temperature with the following structure: Si/SiO_2/10Ta/30IrMn/3.5CoFe/t_1MgO/2.2CoFe/t_2MgO/2.2CoFeB/5Ta/5Ru, where the numbers t_1 and t_2 represent the film thicknesses in nm. They were subsequently postannealed at 300 °C in vacuum ($\sim 1.0 \times 10^{-7}$ Torr) for 30 min with a 1 T field applied in the film plane. The high resolution cross-sectional TEM image in Fig. 1(a) reveals the good structural quality and homogeneity of a DBMTJ film stack

 ©2013 American Physical Society

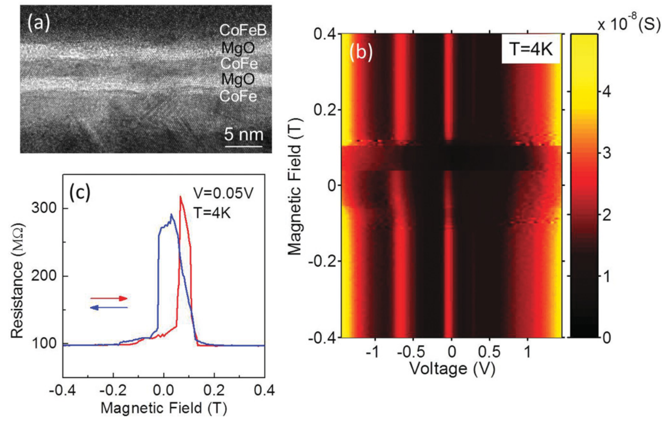

FIG. 1. (Color online) (a) Cross-sectional TEM image of DBMTJ. (b) Three-dimensional plot of differential conductance dI/dV vs voltage and magnetic field. The magnetic field is swept from −0.4 to 0.4 T. (c) Plot of resistance vs magnetic field. Arrows indicate the field sweeping directions.

after the postannealing process. The samples were patterned into ∼40 × 40 nm^2 in size by employing electron-beam and photolithography. A detailed description of the film stack preparation and fabrication can be found in Ref. 21.

III. RESULTS AND DISCUSSIONS

Figure 1(b) shows a typical three-dimentional plot of the differential conductance (dI/dV) as a function of voltage and magnetic field for a DBMTJ with a thicker upper MgO layer ($t_2 = 2.4$ nm) and a thinner lower counterpart ($t_1 = 2.0$ nm). The measurement was conducted at 4 K with a magnetic field applied parallel to the sample surface. Two clear high differential conductance lines (in red) can be readily resolved at −0.05 and −0.68 V, respectively, for the P magnetization alignment, while no such features are present for the AP magnetization alignment. Here, the P configuration has all three magnetic layers magnetized in the same direction, while the AP configuration refers to the scenario where at least the magnetizations of the top CoFeB layer and the middle CoFe magnetic layer are antiparallel to each other (from 0.03 to 0.1 T) as the field is swept from the negative to positive direction. Figure 1(c) shows a full loop of the resistance versus magnetic field.

Figure 2(a) plots the dI/dV curves numerically obtained from I-V curves measured at 4 K for the P and AP magnetization configurations, respectively. In our measurements, tunneling electrons flow from top to bottom electrodes when $V < 0$, and vice versa for $V > 0$. The presence of resonant peaks only for the P configuration is very similar to the spin dependent QW resonant tunneling in a thin Fe layer,[9,11] where the primary resonant peaks also occurred only in the P configuration. Yet our results are different from those observed in Fe/MgO/Fe/MgO/Fe DBMTJs with "hot spots"[22] or thin MgO MTJs with electronic trapping states,[23] where resonant tunneling peaks were present for both P and AP states. To elucidate the important role played by the spin dependent density of states (DOS) in the middle CoFe layer, it is convenient to introduce the differential TMR (dTMR), defined as $\mathrm{dTMR} = (dI_P/dV - dI_{AP}/dV)/(dI_{AP}/dV)$.

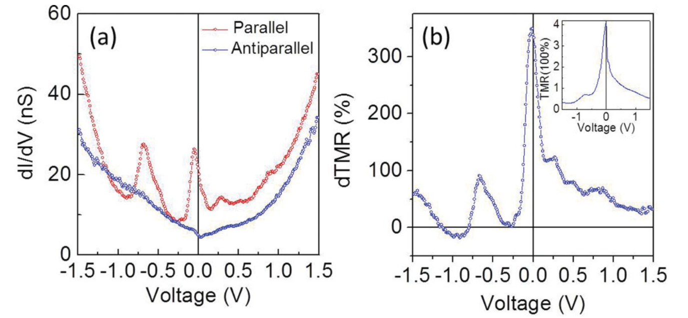

FIG. 2. (Color online) (a) Differential conductance dI/dV curves in the parallel (in red) and antiparallel (in blue) magnetization configurations at 4 K. (b) Differential tunneling magnetoresistance dTMR vs voltage V. $\mathrm{dTMR} = (dI_P/dV_P - dI_{AP}/dV_{AP})/(dI_{AP}/dV_{AP})$. The inset shows TMR vs voltage.

Usually, the spin dependent tunneling matrix-element-weighted DOS (TMEW-DOS) for the majority electrons is greater than that for the minority electrons, resulting in dTMR > 0. In our DBMTJ devices, however, dTMR oscillates with sign changes in the $V < 0$ region, as shown in Fig. 2(b), indicating that the ratio of majority and minority TMEW-DOS varies with the bias voltage. This phenomenon may be attributed to the creation of spin dependent QW states in the middle CoFe layer, which can lead to partially discrete energy levels for the majority spins, whereas continuous energy levels for the minority spins. The majority and minority spins dominate the current tunneling process for the P and AP configurations, respectively, whereas dTMR is determined by the comparison of their respective involved TMEW-DOS; therefore, dTMR peaks are formed when the bias is aligned with a discrete energy level of the majority spins, whereas dips are shown when the bias lies in between two of such levels. The dTMR dip can even become negative as the minority spin DOS is greater than the valley states between discrete majority spin energy levels. The negative dTMR indicates that tunneling is dominated by minority spins rather than majority spins in a certain bias range.

To corroborate our understanding that the observed resonant peaks indeed originate from spin dependent QW states in the middle CoFe layer, we performed first-principles calculations using the layer–Korringa-Kohn-Rostoker method for a junction with the structure of CoFe/MgO(7 ML)/CoFe(10 ML)/MgO(7 ML)/CoFe, with the CoFe, MgO (x,y axis), and MgO (z axis) lattice constants set as 2.84, 2.84, and 2.21 Å, respectively. The CoFe is chosen as the top electrode material for the purpose of computational convenience, since DBMTJs with the CoFe and CoFeB top electrodes show similar behavior. The substitutionally disordered alloy (in which 70% Co and 30% Fe are mixed randomly) is treated with the coherent potential approximation (CPA). The CPA cannot produce k-resolved partial DOS in the reciprocal space, so we invoked an approximation in which after converging the CPA at each energy, the partial DOS for each component (Fe or Co) is calculated using only a single k point, then the result is averaged with the Fe and Co concentrations to approximate the k-resolved partial DOS for that k point (in this case, the $\bar{\Gamma}$ point). The resulting partial DOS does not

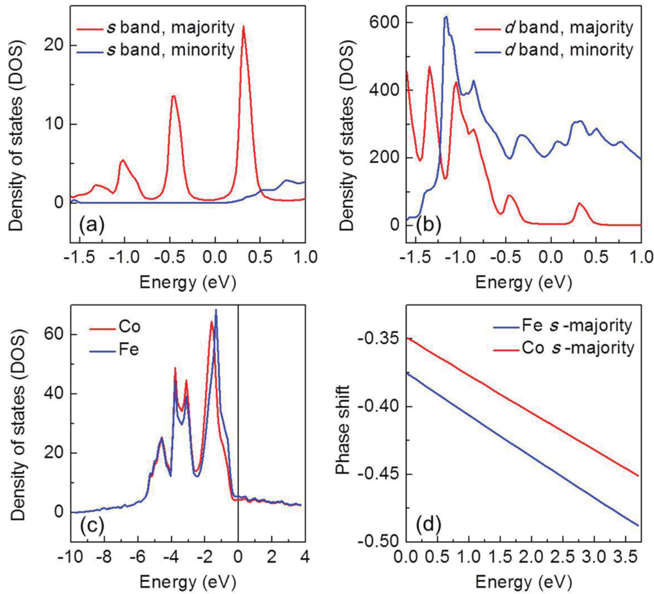

FIG. 3. (Color online) Calculated s- (a) and d- (b) partial density of states at the $\bar{\Gamma}$ point in the middle CoFe layer of a CoFe/MgO(7 ML)/CoFe(10 ML)/MgO(7 ML)/CoFe DBMTJ. (c) The DOS for bulk CoFe on Fe and Co sites. (c) The majority s-phase shifts of Fe and Co potentials in the alloy.

yield the correct total DOS when summed over all k points, but it gives the correct resonant peaks for the QW states. The confinement effect of the MgO layers is tested by increasing the MgO thickness to 11 atomic layers, which has no perceptible effect on the partial DOS. Figures 3(a) and 3(b) show the s and d partial DOS of majority and minority spins at the $\bar{\Gamma}$ point within the middle CoFe layer for the P configuration. Several sharp resonances appear in the s-band DOS for the majority spin: two sharp peaks at about -0.45 and 0.32 eV, and a smaller peak at about -1.0 eV, while no resonances are seen for the minority spin. The two sharp peaks in the s-band DOS also appear in the d-band DOS of the majority spin, indicating a strong s-d hybridization for the QW states. In contrast, no indication of any resonance exists for the minority spin. Since at the $\bar{\Gamma}$ point the dominating tunneling wave function has the Δ_1 character which has the s-band symmetry, the existence of s-band QW resonances in the middle layer should lead to resonant tunneling in the P configuration in which the majority spin of the middle layer matches the Δ_1 tunneling state in the MgO. But in the AP case in which the minority spin of the middle layer is matched with the Δ_1 tunneling state, there should be no resonant tunneling. Note that the first-principles calculations cannot produce resonant peaks near zero bias region, indicating that the resonant peak shown at -0.05 V in Fig. 1(c) may result from magnon assisted tunneling.[8,9,24]

The QW resonances observed here are stronger than those observed in the pure Fe middle layer,[8,9,11–13] indicating a longer spin MFP in CoFe. This result is somewhat counterintuitive since CoFe is an alloy that should contain more disorder, which would seem to destroy electron wave function coherence. To understand why it is possible for CoFe to have a longer majority spin MFP than pure Fe, we also performed the electronic structure calculation of bulk CoFe and show the results in Figs. 3(c) and 3(d). In Fig. 3(c) we show the partial densities of states on the Co and Fe atoms in bulk CoFe. It shows that the Fermi energy in CoFe is well above the d band, unlike in pure Fe where the Fermi energy is inside the d band.[25] Thus the electrons near the Fermi energy are mostly s electrons which have a much longer MFP than the d electrons. Furthermore, in Fig. 3(d) we plot the majority s-phase shifts as a function of the energy for Co and Fe potentials in the CoFe alloy. The difference between the two phase shifts at the Fermi energy is less than 0.03. This would cause a minimal amount of scattering in the alloy. These two factors combined should give a much longer majority spin electron MFP in CoFe than in pure Fe. Indeed, we have measured the resistivities of Fe and CoFe blanket films grown with the same conditions and their values are 19.9 and 9.2 $\mu\Omega \cdot$cm, respectively, indicating a longer electron MFP in the CoFe film.

It is interesting to note that the resonant peaks are only present in the negative bias voltage region in Fig. 2(a). Similar behaviors were observed in Fe/MgO/Fe/MgO/Fe and Fe/MgO/Fe/Cr structures,[9,11] where they were attributed to the asymmetric interfacial structure and the asymmetric potential height of the tunnel barrier, respectively, for electrons tunneling from two different directions. In order to investigate the influence of MgO barrier symmetry on the dI/dV spectra as well as the resonant tunneling mechanism, we have compared the QW resonant tunneling effect in DBMTJs of asymmetric MgO thicknesses with those of symmetric thicknesses.

Figure 4(a) shows the dI/dV spectra for the same device (with asymmetric MgO barrier thicknesses) used in Fig. 2(a), measured at RT for the P and AP magnetization configurations, respectively. Similarly, the resonant peaks are only present in the negative bias voltage region. This phenomenon can be explained using the following schematic model. Figure 4(c) shows the energy potential profiles and schematic illustrations of electron tunneling through DBMTJ for both $V < 0$ and $V > 0$. The left (corresponding to the lower) MgO barrier (2.0 nm) is thinner than the right (corresponding to the upper) one (2.4 nm), resulting in an almost ten times smaller tunneling barrier resistance than that of the right MgO barrier. Consequently, the chemical potential of the middle CoFe layer and the discrete excited states above this are rigidly pinned to the chemical potential of the left CoFe electrode. When $V < 0$, the energies of the electrons that tunnel from the right electrode can line up with the discrete QW states in the middle electrode as the bias voltage drops mostly across the right barrier, thereby giving rise to significant dI/dV oscillations. On the other hand, when $V > 0$, the energy level of the electrons tunneling from the left electrode to the middle one is pinned at the Fermi level of the middle electrode. Therefore no resonant effect is observed. In order to verify our interpretation, we have fabricated DBMTJs with a reversed MgO thickness asymmetry, i.e., the upper (lower) MgO is 2.0 nm (2.4 nm). As expected, pronounced resonant peaks are only observed when $V > 0$, whereas dI/dV spectra are nearly structureless when $V < 0$ (not shown).

In contrast, for DBMTJs with symmetric MgO barrier thicknesses ($t_1 \sim t_2 = 2.4$ nm), we found that clear resonant peaks are present in both negative and positive biases, as shown in Fig. 4(b). In this case, the Fermi level of the middle CoFe

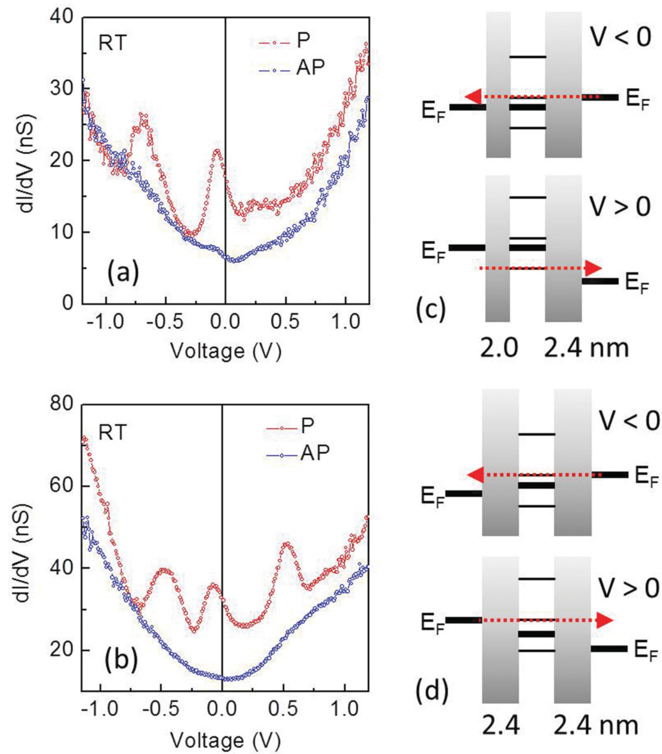

FIG. 4. (Color online) The differential conductance (dI/dV) spectra in the parallel and antiparallel magnetization configurations for different MgO barrier thickness configurations, with the upper and lower MgO thicknesses of (a) 2.4 and 2.0 nm; and (b) 2.4 and 2.4 nm, respectively. (c) and (d) are the potential profiles and schematic illustrations of electron tunneling through DBMTJs shown in (a) and (b), respectively.

layer is not pinned to either of the chemical potentials of the left and right electrodes, but rather lies between them, as shown in Fig. 4(d), because the resistances of two MgO tunnel barriers are similar. Therefore, electrons can tunnel via QW states above E_F for both bias voltage polarities, leading to resonant peaks for both positive and negative voltages.

Figures 5(a) and 5(b) show the bias voltage dependent TMR for samples measured in Figs. 4(a) and 4(b), respectively. Pronounced TMR enhancement can be clearly observed at resonant voltages, although it is still far below the theoretically predicted values of more than 1000%.[26,27] This discrepancy could be due to the fact that the middle CoFe layer (2.2 nm thick) in our DBMTJ is not thin enough for creating a very sharp QW,[26,27] whereas our sputtered middle CoFe layer becomes granular and discontinuous as the film thickness is reduced below 2 nm. Another reason could be that we

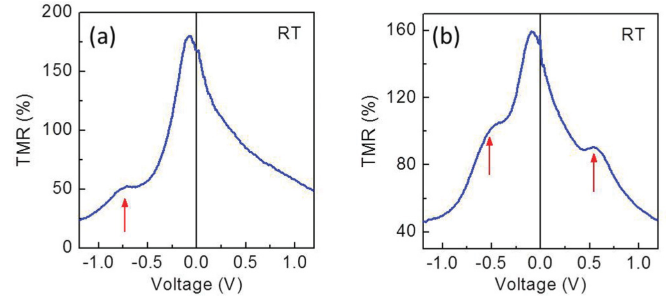

FIG. 5. (Color online) (a),(b) Bias voltage dependence of TMR for the corresponding devices in Figs. 4(a) and 4(b), respectively.

cannot grow atomically flat films over entire junction lateral dimensions[28] for our sputtered DBMTJs, and such inhomogeneity may introduce decoherence which could suppress the creation of the sharp QW states. Therefore, a further reduction of the middle magnetic layer thickness as well as an improved quality of the interface of DBMTJs, such as introducing a CoFeB layer for achieving better homogeneity, are required to realize strong QW effects and thus very high TMR.

IV. SUMMARY

In summary, we have observed spin dependent QW resonant tunneling in the CoFe alloy middle layer of CoFe/MgO/CoFe/MgO/CoFeB DBMTJs. The symmetry of the resonant peak with the bias voltage can be tuned by configuring two MgO barrier thicknesses. Moreover, we have observed pronounced TMR enhancement at resonant voltages. First-principles calculations show that strong QW resonances are possible because in CoFe alloy the Fermi energy lies above the d bands and the difference in the s-phase shift between Co and Fe atomic potentials is small, leading to a longer majority spin electron MFP than that in pure Fe. Our results suggest that it is very promising to create sharp QW states by incorporating a highly (001) textured magnetic alloy middle layer in MgO DBMTJs and thus to achieve very high TMR.

ACKNOWLEDGMENTS

The authors thank Brian Hughes, Larissa Clark, and Leslie Krupp for their help with the experiments, and S. Sanvito and I. Rungger for useful discussions. The authors acknowledge the financial support from DEMA. A portion of this research was conducted at the Center for Nanophase Materials Sciences, sponsored at Oak Ridge National Laboratory by the Scientific User Facilities Division, Office of Basic Energy Sciences, US Department of Energy.

---

*Present address: Data Storage Institute, 5 Engineering Drive 1, Singapore 117608.

[1] T. Miyazaki and N. Tezuka, J. Magn. Magn. Mater. **139**, L231 (1995).
[2] J. S. Moodera, L. R. Kinder, T. M. Wong, and R. Meservey, Phys. Rev. Lett. **74**, 3273 (1995).
[3] S. Yuasa, T. Nagahama, A. Fukushima, Y. Suzuki, and K. Ando, Nature Mater. **3**, 868 (2004).
[4] S. S. P. Parkin, C. Kaiser, A. Panchula, P. M. Rice, B. Hughes, M. Samant, and S.-H. Yang, Nature Mater. **3**, 862 (2004).
[5] X. Zhang, B.-Z. Li, G. Sun, and F.-C. Pu, Phys. Rev. B **56**, 5484 (1997).

[6]T. Kishi and K. Inomata, J. Magn. Soc. Jpn. **23**, 1273 (1999).
[7]Zhong-Yi Lu, X.-G. Zhang, and S. T. Pantelides, Phys. Rev. Lett. **94**, 207210 (2005).
[8]T. Nagahama, S. Yuasa, Y. Suzuki, and E. Tamura, Appl. Phys. Lett. **79**, 4381 (2001).
[9]T. Nozaki, N. Tezuka, and K. Inomata, Phys. Rev. Lett. **96**, 027208 (2006).
[10]Y. Wang, Z.-Y. Lu, X.-G. Zhang, and X.-F. Han, Phys. Rev. Lett. **97**, 087210 (2006).
[11]T. Niizeki, N. Tezuka, and K. Inomata, Phys. Rev. Lett. **100**, 047207 (2008).
[12]F. Greullet, C. Tiusan, F. Montaigne, M. Hehn, D. Halley, O. Bengone, M. Bowen, and W. Weber, Phys. Rev. Lett. **99**, 187202 (2007).
[13]T. Nagahama, S. Yuasa, Y. Suzuki, and E. Tamura, J. Appl. Phys. **91**, 7035 (2002).
[14]W. H. Butler, X.-G. Zhang, and T. C. Schulthess, Phys. Rev. B **63**, 054416 (2001).
[15]J. Mathon and A. Umerski, Phys. Rev. B **63**, 220403(R) (2001).
[16]Bruce A. Gurney, Virgil S. Speriosu, Jean-Pierre Nozieres, Harry Lefakis, Dennis R. Wilhoit, and Omar U. Need, Phys. Rev. Lett. **71**, 4023 (1993).
[17]A. Enders, T. L. Monchesky, K. Myrtle, R. Urban, B. Heinrich, J. Kirschner, X.-G. Zhang, and W. H. Butler, J. Appl. Phys. **89**, 7110 (2001).
[18]X.-G. Zhang and W. H. Butler, Phys. Rev. B **70**, 172407 (2004).
[19]S. Yuasa, T. Nagahama, and Y. Suzuki, Science **297**, 234 (2002).
[20]P. LeClair, B. Hoex, H. Wieldraajjer, J. T. Kohlhepp, H. J. M. Swagten, and W. J. M. de Jonge, Phys. Rev. B **64**, 100406 (2001).
[21]R. S. Liu, S.-H. Yang, X. Jiang, T. Topuria, P. M. Rice, C. Rettner, and S. S. P. Parkin, Appl. Phys. Lett. **100**, 012401 (2012).
[22]D. Herranz, F. G. Aliev, C. Tiusan, M. Hehn, V. K. Dugaev, and J. Barnas, Phys. Rev. Lett. **105**, 047207 (2010).
[23]J. M. Teixeira, J. Ventura, J. P. Araujo, J. B. Sousa, P. Wisniowski, S. Cardoso, and P. P. Freitas, Phys. Rev. Lett. **106**, 196601 (2011).
[24]J. S. Moodera, J. Nowak, and R. J. M. van de Veerdonk, Phys. Rev. Lett. **80**, 2941 (1998).
[25]V. L. Moruzzi, J. F. Janak, and A. R. Williams, *Calculated Electronic Properties of Metals* (Pergamon, New York, 1978).
[26]J. Peralta-Ramos, A. M. Llois, I. Rungger, and S. Sanvito, Phys. Rev. B **78**, 024430 (2008).
[27]A. N. Useinov, J. Kosel, N. Kh. Useinov, and L. R. Tagirov, Phys. Rev. B **84**, 085424 (2011).
[28]A. Iovan, S. Andersson, Yu. G. Naidyuk, A. Vedyaev, B. Dieny, and V. Korenivski, Nano Lett. **8**, 805 (2008).